

1 “Nitrogen demand, availability, and acquisition strategy control plant responses to elevated
2 CO₂ at different scales”

3

4 Evan A. Perkowski^{1,*}, Ezinwanne Ezekannagha¹, Nicholas G. Smith¹

5 ¹Department of Biological Sciences, Texas Tech University, Lubbock, TX

6

7 *Corresponding author:

8 2901 Main St.

9 Lubbock, TX, 79409

10 Email: evan.a.perkowski@ttu.edu

11

12 **ORCIDs:** Evan A. Perkowski (0000-0002-9523-8892), Ezinwanne Ezekannagha (0000-0001-
13 7469-949X), Nicholas G. Smith (0000-0001-7048-4387)

14

15 Total word count: 6436

16 - Introduction: 1298

17 - Methods: 2369

18 - Results: 1027

19 - Discussion: 1742

20

21 Tables: 3

22 Figures: 3

23 Supporting Information: 6 tables, 6 figures

24 **Summary**

- 25 • Plants respond to elevated atmospheric CO₂ concentrations (eCO₂) by reducing
26 photosynthetic capacity, a response that corresponds with increased net photosynthesis,
27 primary productivity, and growth. These responses are commonly assumed to be
28 constrained by nitrogen availability. However, recent work using eco-evolutionary
29 optimality theory suggests that nitrogen demand for building and maintaining
30 photosynthetic enzymes, which optimizes resource allocation to photosynthetic capacity
31 and maximizes allocation to growth, may be a stronger driver of plant responses to eCO₂.
32 • Here, we examined leaf physiological and whole-plant growth responses of *Glycine max*
33 L. (Merr) seedlings subjected to full-factorial combinations of two CO₂, two inoculation,
34 and nine nitrogen fertilization treatments.
35 • Nitrogen fertilization and inoculation did not modify leaf photosynthetic responses to
36 eCO₂. Instead, eCO₂ downregulated the maximum rate of Rubisco carboxylation more
37 strongly than it decreased the maximum rate of electron transport for RuBP regeneration,
38 increasing net photosynthesis rates by approaching optimal coordination. Increasing
39 fertilization enhanced positive whole-plant responses to eCO₂ due to increased nitrogen
40 uptake and reduced nitrogen acquisition costs.
41 • Patterns expected from eco-evolutionary optimality theory determined leaf
42 photosynthetic responses to eCO₂, while nitrogen availability constrained whole-plant
43 responses. Results suggest that nitrogen availability and demand each drive plant
44 responses to eCO₂, though operate at different scales

45

46 **Plain Language Summary**

47 Plant responses to elevated CO₂ are commonly assumed to be regulated by nitrogen availability.
48 However, recent work suggests that demand for building and maintaining photosynthetic
49 enzymes may be a stronger predictor of plant responses to elevated CO₂. Here, we reconcile
50 these competing ideas, showing that nitrogen demand determines leaf responses while nitrogen
51 availability controls whole-plant responses to elevated CO₂.

52

53 **Keywords**

54 acclimation, eco-evolutionary optimality, growth chamber, least-cost theory, nitrogen acquisition
55 strategy, photosynthesis, plant functional ecology, whole-plant growth

56

57 **Introduction**

58 Complex carbon and nitrogen cycles regulate terrestrial ecosystems. Terrestrial biosphere
59 models, which are beginning to include coupled carbon and nitrogen cycles (Davies-Barnard *et*
60 *al.*, 2020; Kou-Giesbrecht *et al.*, 2023), must accurately represent these cycles under different
61 environmental scenarios to reliably simulate carbon and nitrogen fluxes (Hungate *et al.*, 2003;
62 Prentice *et al.*, 2015). While including coupled carbon and nitrogen cycles was intended to
63 improve terrestrial biosphere model reliability, the role of nitrogen availability and nitrogen
64 acquisition strategy on leaf and whole plant responses to increasing atmospheric CO₂
65 concentrations remains uncertain (Davies-Barnard *et al.*, 2020), contributing to divergent future
66 carbon and nitrogen flux simulations across terrestrial biosphere models (Friedlingstein *et al.*,
67 2014; Wieder *et al.*, 2015; Arora *et al.*, 2020; Meyerholt *et al.*, 2020).

68 Over the past few decades, numerous studies have revealed consistent leaf and whole-
69 plant responses to elevated CO₂ (eCO₂). At the leaf level, C₃ plants grown under eCO₂ exhibit
70 increased net photosynthesis rates compared to plants grown under ambient CO₂ (aCO₂)
71 (Ainsworth & Long, 2005; Lee *et al.*, 2011; Poorter *et al.*, 2022). These patterns correspond with
72 reduced mass- and area-based leaf nitrogen content, increased leaf mass per area, reduced
73 stomatal conductance, and reduced photosynthetic capacity, yielding increased photosynthetic
74 nitrogen-use efficiency and water-use efficiency (Curtis, 1996; Drake *et al.*, 1997; Ainsworth &
75 Long, 2005; Ainsworth & Rogers, 2007; Lee *et al.*, 2011; Pastore *et al.*, 2019; Poorter *et al.*,
76 2022). At the whole-plant level, C₃ plants grown under eCO₂ exhibit increased total leaf area,
77 which supports greater net primary productivity and total biomass compared to plants grown
78 under aCO₂ (Ainsworth *et al.*, 2002; Ainsworth & Rogers, 2007; Poorter *et al.*, 2022).

79 Despite consistent plant responses to eCO₂ documented across experiments, mechanisms
80 that drive these responses remain unresolved. Some have hypothesized that plant responses to
81 eCO₂ are constrained by nitrogen availability, as nitrogen availability limits net primary
82 productivity globally (LeBauer & Treseder, 2008). The progressive nitrogen limitation
83 hypothesis predicts that eCO₂ increases plant nitrogen uptake to support greater net primary
84 productivity, which causes nitrogen availability to decline over time (Luo *et al.*, 2004). The

85 hypothesis predicts that this response should enhance positive effects of eCO₂ on net primary
86 productivity and growth under eCO₂ over short time scales that dampen with time as nitrogen
87 becomes more limiting and stored in longer-lived tissues. Growth responses to eCO₂ expected
88 from the progressive nitrogen limitation hypothesis have received some support from free-air
89 CO₂ enrichment experiments (Reich *et al.*, 2006; Norby *et al.*, 2010), though these patterns are
90 not consistently observed (Finzi *et al.*, 2006; Moore *et al.*, 2006; Liang *et al.*, 2016).

91 Assuming positive relationships between soil nitrogen availability, leaf nitrogen content,
92 and photosynthetic capacity (Field & Mooney, 1986; Evans, 1989), the progressive nitrogen
93 limitation hypothesis implies that reductions in nitrogen availability over time might explain why
94 C₃ plants grown under eCO₂ exhibit decreased leaf nitrogen content and photosynthetic capacity.
95 However, free-air CO₂ enrichment experiments show that reductions in leaf nitrogen content and
96 photosynthetic capacity due to eCO₂ are decoupled from changes in nitrogen availability (Crous
97 *et al.*, 2010; Lee *et al.*, 2011; Pastore *et al.*, 2019). Additionally, aboveground conditions that
98 alter the demand for building and maintaining photosynthetic enzymes may be a stronger
99 determinant of variance in leaf nitrogen and photosynthetic capacity across environmental
100 gradients (Dong *et al.*, 2017, 2020, 2022a; Paillassa *et al.*, 2020; Peng *et al.*, 2021; Waring *et al.*,
101 2023). Thus, leaf photosynthetic responses to eCO₂ may be a product of altered demand to build
102 and maintain photosynthetic enzymes and not due to changes in nitrogen availability.

103 Eco-evolutionary optimality theory provides a framework for understanding how demand
104 for building and maintaining photosynthetic enzymes dictates leaf photosynthetic responses to
105 eCO₂ (Harrison *et al.*, 2021). Merging photosynthetic least-cost (Wright *et al.*, 2003; Prentice *et*
106 *al.*, 2014) and optimal coordination (Chen *et al.*, 1993; Maire *et al.*, 2012) theories, eco-
107 evolutionary optimality theory posits that reduced leaf nitrogen allocation due to eCO₂ is the
108 downstream result of a stronger downregulation in the maximum rate of Ribulose-1,5-
109 bisphosphate (RuBP) carboxylase/oxygenase (Rubisco) carboxylation (V_{cmax}) than the maximum
110 rate of electron transport for RuBP regeneration (J_{max}), which reduces leaf nitrogen demand for
111 building and maintaining photosynthetic enzymes. The theory predicts that plants should
112 optimize leaf nitrogen allocation to photosynthetic capacity to make more efficient use of
113 available light while avoiding overinvestment in Rubisco, which has high nitrogen costs to build
114 and maintain (Evans, 1989; Evans & Clarke, 2019). Such responses to eCO₂ increase
115 photosynthetic nitrogen-use efficiency and increase net photosynthesis rates through increasingly

116 equal co-limitation of Rubisco carboxylation and electron transport for RuBP regeneration (Chen
117 *et al.*, 1993; Maire *et al.*, 2012; Wang *et al.*, 2017; Smith *et al.*, 2019). The expected optimal leaf
118 response to eCO₂ has received some empirical support (Crous *et al.*, 2010; Lee *et al.*, 2011;
119 Smith & Keenan, 2020; Dong *et al.*, 2022b), though no studies have connected these patterns
120 with concurrently measured whole-plant responses.

121 The eco-evolutionary optimality hypothesis deviates from the progressive nitrogen
122 limitation hypothesis by indicating that changes in leaf nitrogen demand to build and maintain
123 photosynthetic enzymes drive leaf-level responses to eCO₂ independent of changes in soil
124 nitrogen availability. However, the eco-evolutionary optimality hypothesis does not discount the
125 role of soil nitrogen availability on whole-plant responses to eCO₂, where the expected optimal
126 strategy in response to eCO₂ is to allocate surplus nitrogen not needed to satisfy demand to build
127 and maintain photosynthetic enzymes toward the construction of a greater quantity of optimally
128 coordinated leaves and other plant organs. Thus, whether patterns expected from the progressive
129 nitrogen limitation hypothesis or eco-evolutionary optimality theory control plant responses to
130 eCO₂ may be a matter of scale, where leaf nitrogen demand to build and maintain photosynthetic
131 enzymes determines leaf-level responses to eCO₂ and nitrogen availability regulates whole-plant
132 responses to eCO₂.

133 Plants allocate carbon belowground in exchange for nutrients through different nutrient
134 acquisition strategies, including direct uptake pathways or symbioses with mycorrhizal fungi and
135 symbiotic nitrogen-fixing bacteria. Carbon costs to acquire nitrogen, or the amount of carbon
136 plants allocate belowground per unit of nitrogen acquired, vary in species with different nitrogen
137 acquisition strategies and are dependent on environmental factors such as atmospheric CO₂,
138 temperature, light availability, and nutrient availability (Brzostek *et al.*, 2014; Terrer *et al.*, 2018;
139 Perkowski *et al.*, 2021). Therefore, it is important to consider nitrogen acquisition strategy when
140 examining the effects of nitrogen availability on plant responses to eCO₂. Few studies account
141 for acquisition strategy when considering the role of nitrogen availability on leaf and whole-plant
142 responses to eCO₂ (Terrer *et al.*, 2018; Smith & Keenan, 2020). Such studies found that nitrogen
143 acquisition strategies with reduced carbon costs to acquire nitrogen may buffer the effect of
144 nitrogen limitation at the whole-plant level (Terrer *et al.*, 2018), but leaf-level responses remain
145 inconsistent (Terrer *et al.*, 2018; Smith & Keenan, 2020).

146 Here, *Glycine max* L. (Merr.) seedlings were grown under full-factorial combinations of
147 two CO₂ concentrations, two inoculation treatments, and nine soil nitrogen fertilization
148 treatments to reconcile the role of nitrogen availability and demand on plant responses to eCO₂.
149 We used this experimental setup to test the following hypotheses:

- 150 (1) Following eco-evolutionary optimality theory, eCO₂ will downregulate V_{cmax} more
151 strongly than J_{max} , increasing the ratio of J_{max} to V_{cmax} and allowing increased net
152 photosynthesis rates to approach equal co-limitation of Rubisco carboxylation and
153 electron transport for RuBP regeneration. Leaf photosynthetic responses to eCO₂ will be
154 independent of nitrogen fertilization and inoculation treatment.
- 155 (2) Following the progressive nitrogen limitation hypothesis, nitrogen fertilization will
156 enhance the positive effect of eCO₂ on total leaf area and total biomass due to increased
157 plant nitrogen uptake and reduced carbon costs to acquire nitrogen. Inoculation with
158 symbiotic nitrogen-fixing bacteria will enhance positive growth responses to eCO₂.
159 However, these responses will only be apparent under low nitrogen fertilization, where
160 individuals will invest more strongly in symbiotic nitrogen fixation.

161

162 Methods

163 Seed treatments and experimental design

164 *Glycine max* seeds were planted in 144 6-liter surface sterilized pots (NS-600, Nursery Supplies,
165 Orange, CA, USA) containing a steam-sterilized 70:30 volume: volume mix of *Sphagnum* peat
166 moss (Premier Horticulture, Quakertown, PA, USA) to sand (Pavestone, Atlanta, GA, USA).
167 Before planting, all *G. max* seeds were surface sterilized in 2% sodium hypochlorite for 3
168 minutes, followed by three 3-minute washes with ultrapure water (MilliQ 7000; MilliporeSigma,
169 Burlington, MA USA). Subsets of surface-sterilized seeds were inoculated with *Bradyrhizobium*
170 *japonicum* (Verdesian N-Dure™ Soybean, Cary, NC, USA) in a slurry following manufacturer
171 recommendations (3.12 g inoculant and 241 g ultrapure water per 1 kg seed).

172 Seventy-two pots were randomly planted with surface-sterilized seeds inoculated with *B.*
173 *japonicum*, while the remaining 72 pots were planted with surface-sterilized uninoculated seeds.
174 Thirty-six pots in each inoculation treatment were placed in one of two atmospheric CO₂
175 treatments (420, 1000 $\mu\text{mol mol}^{-1}$ CO₂). Plants in each unique inoculation-by-CO₂ treatment
176 combination received one of nine nitrogen fertilization treatments equivalent to 0 (0 mM), 35

177 (2.5 mM), 70 (5 mM), 105 (7.5 mM), 140 (10 mM), 210 (15 mM), 280 (20 mM), 350 (25 mM),
178 or 630 ppm (45 mM) N. Nitrogen fertilization treatments were created using a modified
179 Hoagland's solution (Hoagland & Arnon, 1950) designed to keep concentrations of all other
180 macronutrients and micronutrients equivalent across treatments (Table S1). Plants received the
181 same nitrogen fertilization treatment twice per week in 150 mL doses as topical agents to the soil
182 surface.

183

184 *Growth chamber conditions*

185 Plants were randomly placed in one of six Percival LED-41L2 growth chambers (Percival
186 Scientific Inc., Perry, IA, USA) over two experimental iterations due to chamber space
187 limitation. The first iteration included all plants grown under eCO₂, while the second included all
188 plants grown under aCO₂. Average (\pm SD) CO₂ concentrations across chambers throughout the
189 experiment were $439 \pm 5 \text{ } \mu\text{mol mol}^{-1}$ CO₂ for the ambient treatment and $989 \pm 4 \text{ } \mu\text{mol mol}^{-1}$ CO₂
190 for the elevated treatment.

191 Daytime growth conditions were simulated using a 16-hour photoperiod, with incoming
192 light radiation set to chamber maximum (mean \pm SD: $1230 \pm 12 \text{ } \mu\text{mol m}^{-2} \text{ s}^{-1}$ across chambers), air
193 temperature set to 25°C, and relative humidity set to 50%. The remaining 8-hour period
194 simulated nighttime growing conditions, with incoming light radiation set to $0 \text{ } \mu\text{mol m}^{-2} \text{ s}^{-1}$,
195 chamber temperature set to 17°C, and relative humidity set to 50%. Transitions between daytime
196 and nighttime growing conditions were simulated by ramping incoming light radiation in 45-
197 minute increments and temperature in 90-minute increments over 3 hours (Table S2).

198 Plants grew under average (\pm SD) daytime light intensity of $1049 \pm 27 \text{ } \mu\text{mol m}^{-2} \text{ s}^{-1}$,
199 including ramping periods. In the eCO₂ iteration, plants grew under $24.0 \pm 0.2^\circ\text{C}$ during the day,
200 $16.4 \pm 0.8^\circ\text{C}$ during the night, and $51.6 \pm 0.4\%$ relative humidity. In the aCO₂ iteration, plants grew
201 under $23.9 \pm 0.2^\circ\text{C}$ during the day, $16.0 \pm 1.4^\circ\text{C}$ during the night, and $50.3 \pm 0.2\%$ relative humidity.
202 Any differences in climate conditions across the six chambers were accounted for by shuffling
203 the same group of plants throughout the growth chambers. This process was done by iteratively
204 moving the group of plants on the top rack of a chamber to the bottom rack of the same chamber
205 while simultaneously moving the group of plants on the bottom rack of a chamber to the top rack
206 of the adjacent chamber. Plants were moved within and across chambers daily during each
207 experiment iteration.

208

209 *Leaf gas exchange measurements*

210 Leaf gas exchange measurements were collected on the seventh week of development, before the
211 onset of reproduction. All gas exchange measurements were collected on the center leaf of the
212 most recent fully expanded trifoliate leaf set using LI-6800 portable photosynthesis machines
213 configured with a 6800-01A fluorometer head and 6 cm² aperture (LI-COR Biosciences,
214 Lincoln, NE, USA). Specifically, net photosynthesis rates (A_{net} ; $\mu\text{mol m}^{-2} \text{s}^{-1}$), stomatal
215 conductance rates (g_{sw} ; $\text{mol m}^{-2} \text{s}^{-1}$), and intercellular CO₂ concentrations (C_i ; $\mu\text{mol mol}^{-1}$) were
216 measured across a range of atmospheric CO₂ concentrations (i.e., an A_{net}/C_i curve) using the
217 Dynamic Assimilation™ Technique. The Dynamic Assimilation™ Technique corresponds well
218 with traditional steady-state A_{net}/C_i curves in *G. max* (Saathoff & Welles, 2021). A_{net}/C_i curves
219 were generated along a reference CO₂ ramp down from 420 $\mu\text{mol mol}^{-1}$ CO₂ to 20 $\mu\text{mol mol}^{-1}$
220 CO₂, followed by a ramp up from 420 $\mu\text{mol mol}^{-1}$ CO₂ to 1620 $\mu\text{mol mol}^{-1}$ CO₂ after a 90-
221 second wait period at 420 $\mu\text{mol mol}^{-1}$ CO₂. The ramp rate for each curve was set to 200 μmol
222 $\text{mol}^{-1} \text{min}^{-1}$, logging every five seconds, generating 96 data points per response curve. All A_{net}/C_i
223 curves were conducted after A_{net} and g_{sw} stabilized in a LI-6800 cuvette set to a 500 mol s^{-1} flow
224 rate, 10000 rpm mixing fan speed, 1.5 kPa vapor pressure deficit, 25°C leaf temperature, 2000
225 $\mu\text{mol m}^{-2} \text{s}^{-1}$ incoming light radiation, and initial reference CO₂ set to 420 $\mu\text{mol mol}^{-1}$.

226 Snapshot A_{net} measurements were extracted from each A_{net}/C_i curve, both at a common
227 CO₂ concentration, 420 $\mu\text{mol mol}^{-1}$ CO₂ ($A_{\text{net},420}$; $\mu\text{mol m}^{-2} \text{s}^{-1}$), and growth CO₂ concentration,
228 420 and 1000 $\mu\text{mol mol}^{-1}$ CO₂ ($A_{\text{net,growth}}$; $\mu\text{mol m}^{-2} \text{s}^{-1}$). Dark respiration (R_d ; $\mu\text{mol m}^{-2} \text{s}^{-1}$)
229 measurements were collected on the same leaf used to generate A_{net}/C_i curves following at least
230 30 minutes of darkness. Measurements were collected on a 5-second log interval for 60 seconds
231 after the leaf stabilized in a LI-6800 cuvette set to a 500 mol s^{-1} flow rate, 10000 rpm mixing fan
232 speed, 1.5 kPa vapor pressure deficit, 25°C leaf temperature, and 420 $\mu\text{mol mol}^{-1}$ reference CO₂
233 concentration (regardless of CO₂ treatment), with incoming light radiation set to 0 $\mu\text{mol m}^{-2} \text{s}^{-1}$.
234 A single dark respiration value was determined for each leaf by calculating the mean dark
235 respiration value across the logging interval.

236

237 *A/C_i curve-fitting and parameter estimation*

238 A_{net}/C_i curves were fit using the 'fitaci' function in the 'plantecophys' R package(Duursma,
239 2015). This function estimates the maximum rate of Rubisco carboxylation (V_{cmax} ; $\mu\text{mol m}^{-2} \text{s}^{-1}$)
240 and maximum rate of electron transport for RuBP regeneration (J_{max} ; $\mu\text{mol m}^{-2} \text{s}^{-1}$) based on the
241 Farquhar et al. (1980) biochemical model of C₃ photosynthesis. Triose phosphate utilization
242 (TPU) limitation was included as an additional rate-limiting step after visually observing clear
243 TPU limitation for most curves. All curve fits included measured dark respiration values. As
244 A_{net}/C_i curves were generated using a common leaf temperature (25°C), curves were fit using
245 Michaelis-Menten coefficients for Rubisco affinity to CO₂ (K_c ; $\mu\text{mol mol}^{-1}$) and O₂ (K_o ; mmol
246 mol^{-1}), and the CO₂ compensation point (T^* ; $\mu\text{mol mol}^{-1}$) reported in Bernacchi et al. (2001).
247 Specifically, K_c was set to 404.9 $\mu\text{mol mol}^{-1}$, K_o was set to 278.4 $\mu\text{mol mol}^{-1}$, and T^* was set to
248 42.75 $\mu\text{mol mol}^{-1}$. V_{cmax} , J_{max} , and R_d estimates are referenced throughout the rest of the paper as
249 V_{cmax25} , J_{max25} , and R_{d25} .

250

251 *Leaf trait measurements*

252 The leaf used for A_{net}/C_i curves and dark respiration measurements was harvested immediately
253 following gas exchange measurements. Images of each focal leaf were curated using a flat-bed
254 scanner to determine fresh leaf area using the 'LeafArea' R package (Katabuchi, 2015), which
255 automates leaf area calculations using ImageJ software (Schneider *et al.*, 2012). Post-processed
256 images were visually assessed to check against errors in the automation process. Each leaf was
257 dried at 65°C for at least 48 hours, weighed, and ground until homogenized. Leaf mass per area
258 (M_{area} ; g m^{-2}) was calculated as the ratio of dry leaf biomass to fresh leaf area. Leaf nitrogen
259 content (N_{mass} ; gN g^{-1}) was quantified using a subsample of ground and homogenized leaf tissue
260 through elemental combustion (Costech-4010, Costech, Inc., Valencia, CA, USA). Leaf nitrogen
261 content per unit leaf area (N_{area} ; gN m^{-2}) was calculated by multiplying N_{mass} and M_{area} .
262 Photosynthetic nitrogen-use efficiency ($PNUE_{\text{growth}}$; $\mu\text{mol CO}_2 \text{ g}^{-1} \text{ N s}^{-1}$) was estimated as the
263 ratio of $A_{\text{net,growth}}$ to N_{area} . Chlorophyll content was extracted from a second leaf in the same
264 trifoliolate leaf set as the leaf used to generate A_{net}/C_i curves and quantified using methods
265 described in Barnes *et al.* (1992) and Wellburn (1994). Detailed methods for chlorophyll
266 extractions are included in the *Supplemental Material*.

267 Subsamples of ground and homogenized leaf tissue were sent to the University of
268 California-Davis Stable Isotope Facility to determine leaf δ¹³C and δ¹⁵N using an elemental

269 analyzer (Elementar vario MICRO cube elemental analyzer; Elementar Analysensysteme GmbH,
270 Langenselbold, Germany) interfaced to an isotope ratio mass spectrometer (PDZ Europa 20-20
271 Isotope Ratio Mass Spectrometer, Sercon Ltd., Chestshire, UK). Leaf $\delta^{13}\text{C}$ was used to estimate
272 the ratio of leaf intercellular CO₂ concentration to atmospheric CO₂ concentration (χ , unitless),
273 summarized in the *Supplemental Material*. The percent of leaf nitrogen derived from the
274 atmosphere (%N_{dfa}; %) was estimated following Andrews et al. (2011):

$$275 \quad \%N_{dfa} = \frac{\delta^{15}\text{N}_{direct} - \delta^{15}\text{N}_{sample}}{\delta^{15}\text{N}_{direct} - \delta^{15}\text{N}_{fixation}} \quad (1)$$

276 where $\delta^{15}\text{N}_{direct}$ refers to $\delta^{15}\text{N}$ from plants that acquired nitrogen only through direct uptake,
277 $\delta^{15}\text{N}_{sample}$ refers to an individual's leaf $\delta^{15}\text{N}$, and $\delta^{15}\text{N}_{fixation}$ refers to $\delta^{15}\text{N}$ from individuals
278 entirely reliant on nitrogen fixation. $\delta^{15}\text{N}_{direct}$ was calculated as the mean leaf $\delta^{15}\text{N}$ of
279 uninoculated individuals for each nitrogen fertilization-by-CO₂ treatment combination. Any
280 individual with visual evidence of root nodule formation or nodule initiation was omitted from
281 $\delta^{15}\text{N}_{direct}$. $\delta^{15}\text{N}_{fixation}$ was calculated for each CO₂ treatment using the mean leaf $\delta^{15}\text{N}$ of
282 inoculated individuals that received 0 ppm N. $\delta^{15}\text{N}_{fixation}$ was not calculated for each nitrogen
283 fertilization-by-CO₂ treatment combination due to decreased reliance on symbiotic nitrogen
284 fixation with increasing nitrogen fertilization (Rastetter et al., 2001; Andrews et al., 2011;
285 Perkowski et al., 2021).

286

287 *Whole-plant measurements*

288 All individuals were harvested, and biomass of major organ types (leaves, stems, roots, and
289 nodules when present) were separated immediately following gas exchange measurements. Fresh
290 leaf area of all harvested leaves was measured using a LI-3100C (LI-COR Biosciences, Lincoln,
291 Nebraska, USA). Total fresh leaf area (cm²) was calculated as the sum of all leaf areas, including
292 the leaf used for gas exchange and chlorophyll extractions. Harvested material was separately
293 dried in an oven set to 65°C for at least 48 hours to a constant mass, weighed, and ground to
294 homogeneity. Leaves and root nodules were ground using a mortar and pestle, while stems and
295 roots were ground using an E3300 Single Speed Mini Cutting Mill (Eberbach Corp., MI, USA).
296 Total biomass (g) was calculated as the sum of dry leaf, stem, root, and root nodule biomass.
297 Carbon and nitrogen content was measured for each organ type through elemental combustion
298 (Costech-4010, Costech, Inc., Valencia, CA, USA) using ground and homogenized organ tissue

299 subsamples. The ratio of root nodule biomass to root biomass was calculated as an additional
300 indicator of investment toward nitrogen fixation.

301 Carbon costs to acquire nitrogen were quantified as the ratio of belowground carbon
302 biomass to total nitrogen biomass (N_{cost} ; gC gN⁻¹) (Perkowski *et al.*, 2021). Belowground carbon
303 biomass (C_{bg} ; gC) was calculated as the sum of root and root nodule carbon biomass. Root
304 carbon biomass and root nodule carbon biomass were calculated as the product of the organ
305 biomass and respective organ carbon content. Total nitrogen biomass (N_{wp} ; gN) was calculated
306 as the sum of total leaf, stem, root, and root nodule nitrogen biomass. Leaf, stem, root, and root
307 nodule nitrogen biomass was calculated as the product of the organ biomass and respective organ
308 nitrogen content. This calculation does not account for additional carbon costs associated with
309 respiration, root exudation, or root turnover and may underestimate carbon costs to acquire
310 nitrogen (Perkowski *et al.*, 2021).

311

312 *Statistical analyses*

313 Uninoculated plants with substantial root nodule formation (root nodule biomass: root biomass
314 values greater than 0.05 g g⁻¹) were removed from analyses assuming that plants were either
315 incompletely sterilized or were colonized by neighboring plants in the chamber. This decision
316 resulted in the removal of sixteen plants from the analysis: two plants in the eCO₂ treatment that
317 received 35 ppm N, three plants in the eCO₂ treatment that received 70 ppm N, one plant in the
318 eCO₂ treatment that received 210 ppm N, two plants in the eCO₂ treatment that received 280
319 ppm N, two plants in the aCO₂ treatment that received 0 ppm N, three plants in the aCO₂
320 treatment that received 70 ppm N, two plants in the aCO₂ treatment that received 105 ppm N,
321 and one plant in the aCO₂ treatment that received 280 ppm N.

322 A series of linear mixed-effects models were built to investigate the impacts of CO₂
323 concentration, nitrogen fertilization, and inoculation on *G. max* leaf nitrogen allocation, gas
324 exchange, whole-plant growth, and investment in nitrogen fixation. All models included CO₂
325 treatment as a categorical fixed effect, inoculation treatment as a categorical fixed effect, and
326 nitrogen fertilization as a continuous fixed effect, with all possible interaction terms between all
327 three fixed effects also included. Models accounted for climatic differences between chambers
328 across experiment iterations by including a random intercept term that nested the starting
329 chamber rack by CO₂ treatment. Models with this independent variable structure were created for

330 each of the following dependent variables: N_{area} , M_{area} , N_{mass} , Chl_{area} , $A_{\text{net},420}$, $A_{\text{net,growth}}$, $V_{\text{cmax}25}$,
331 $J_{\text{max}25}$, $J_{\text{max}25}:V_{\text{cmax}25}$, $R_{\text{d}25}$, $PNUE_{\text{growth}}$, χ , total leaf area, total biomass, N_{cost} , C_{bg} , N_{wp} , $\%N_{\text{dfa}}$,
332 root nodule biomass: root biomass, root nodule biomass, and root biomass.

333 Shapiro-Wilk tests of normality were used to assess whether linear mixed-effects models
334 satisfied residual normality assumptions. Models for N_{area} , N_{mass} , Chl_{area} , $A_{\text{net},420}$, $A_{\text{net,growth}}$,
335 $V_{\text{cmax}25}$, $J_{\text{max}25}$, $J_{\text{max}25}:V_{\text{cmax}25}$, $R_{\text{d}25}$, $PNUE_{\text{growth}}$, χ , total leaf area, and N_{cost} each satisfied residual
336 normality assumptions without data transformation. Models for M_{area} , total biomass, and C_{bg}
337 satisfied residual normality assumptions with a natural log data transformation. Models for N_{wp} ,
338 root nodule biomass: root biomass, root nodule biomass, root biomass, and $\%N_{\text{dfa}}$ satisfied
339 residual normality assumptions with a square root data transformation.

340 In all models, the ‘lmer’ function in the ‘lme4’ R package (Bates *et al.*, 2015) was used to
341 fit each model, and the ‘Anova’ function in the ‘car’ R package (Fox & Weisberg, 2019) was
342 used to calculate Type II Wald's χ^2 and determine the significance ($\alpha=0.05$) of each fixed effect
343 coefficient. The ‘emmeans’ R package (Lenth, 2019) was used to conduct post-hoc comparisons
344 using Tukey's tests, where degrees of freedom were approximated using the Kenward-Roger
345 approach (Kenward & Roger, 1997). Trendlines and error ribbons representing the 95%
346 confidence intervals were drawn in all figures using ‘emmeans’ outputs across the range in
347 nitrogen fertilization values. All analyses and plots were conducted in R version 4.1.0 (R Core
348 Team, 2021). Model results for $PNUE_{\text{growth}}$, χ , C_{bg} , N_{wp} , root nodule biomass: root biomass, root
349 nodule biomass, and root biomass are reported in the *Supplemental Material* (Tables S3-S6;
350 Figs. S3-S6).

351

352 Results

353 Leaf nitrogen content

354 eCO₂ reduced N_{area} , N_{mass} , and Chl_{area} by 29%, 50%, and 31%, respectively, and increased M_{area}
355 by 44% ($p<0.001$ in all cases; Table 1). Interactions between nitrogen fertilization and CO₂
356 ($p<0.05$ in all cases; Table 1) indicated that the positive effects of increasing nitrogen
357 fertilization on N_{area} , N_{mass} , and M_{area} ($p<0.001$ in all cases; Table 1) were stronger under aCO₂
358 than eCO₂ (Tukey test of the nitrogen fertilization-trait slope between CO₂: $p<0.05$ in all cases).
359 These responses resulted in a stronger reduction in N_{area} and N_{mass} and a stronger increase in M_{area}
360 under eCO₂ with increasing nitrogen fertilization than aCO₂ (Fig. S1). Nitrogen fertilization did

361 not modify reductions in Chl_{area} due to eCO₂ (Tukey test of the nitrogen fertilization- Chl_{area} slope
362 between CO₂ treatments: $p>0.05$).

363 An interaction between inoculation and CO₂ ($p<0.05$; Table 1) indicated that reductions
364 in N_{area} due to eCO₂ were stronger in uninoculated plants (36% reduction; Tukey test of the CO₂
365 effect in uninoculated plants: $p<0.001$) than inoculated plants (22% reduction; Tukey test of the
366 CO₂ effect in inoculated plants: $p<0.001$). Inoculation did not modify N_{mass} , M_{area} , or Chl_{area}
367 responses to eCO₂ (CO₂-by-inoculation interaction: $p>0.05$ in all cases; Table 1). However, an
368 interaction between nitrogen fertilization and inoculation ($p<0.05$ in all cases; Table 1; Figs. 1a-
369 d) indicated that positive effects of increasing nitrogen fertilization on N_{area} , N_{mass} , M_{area} , and
370 Chl_{area} ($p<0.001$ in all cases; Table 1) were stronger in uninoculated plants compared to
371 inoculated plants (Tukey test of the nitrogen fertilization-trait slope between inoculation
372 treatments: $p<0.05$ in all cases).

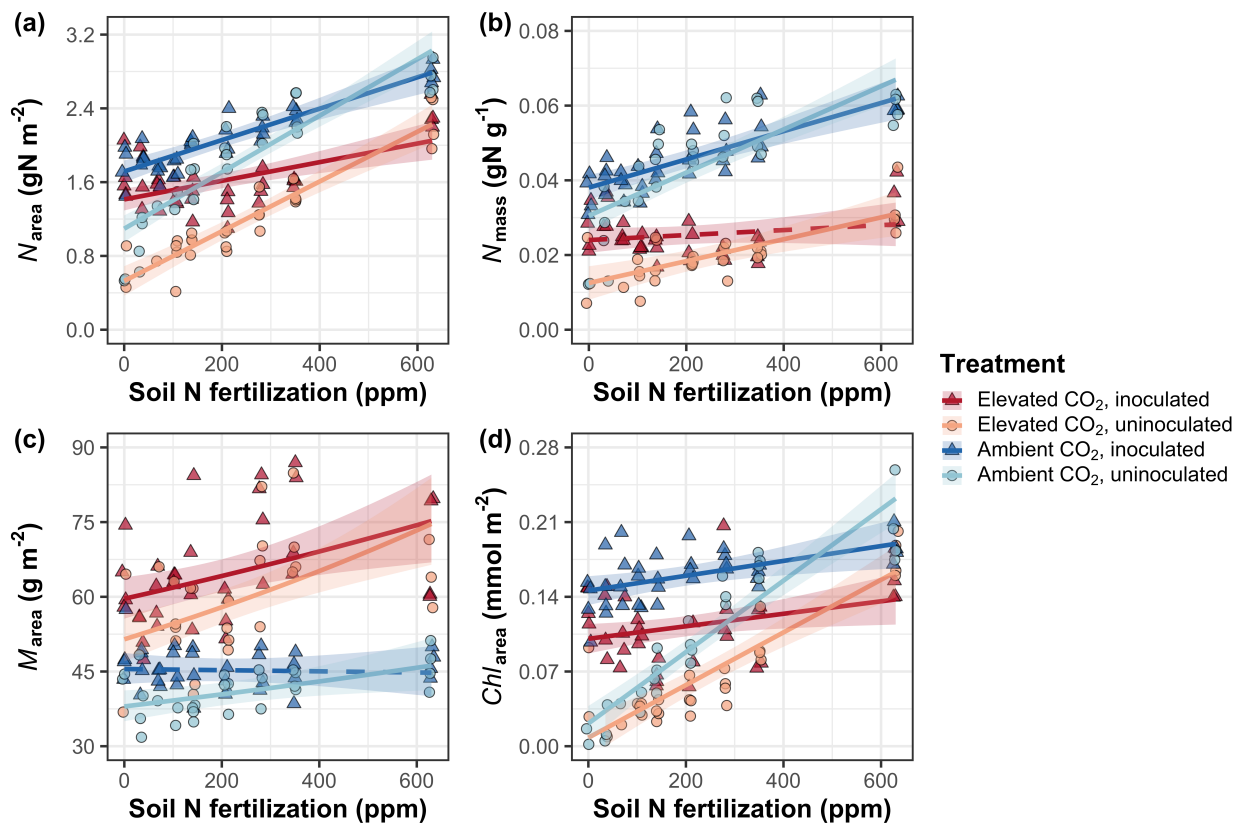
373

374 **Table 1** Effects of CO₂ concentration, inoculation, and nitrogen fertilization on leaf nitrogen allocation*

		<i>N_{area}</i>		<i>N_{mass}</i>		<i>M_{area}^a</i>		<i>Chl_{area}</i>	
	df	χ^2	<i>p</i>	χ^2	<i>p</i>	χ^2	<i>p</i>	χ^2	<i>p</i>
CO ₂	1	155.908	<0.001	272.362	<0.001	151.319	<0.001	69.233	<0.001
Inoculation (I)	1	86.029	<0.001	15.576	<0.001	19.158	<0.001	136.341	<0.001
N fertilization (N)	1	316.408	<0.001	106.659	<0.001	21.440	<0.001	163.111	<0.001
CO ₂ *I	1	4.729	0.030	2.025	0.155	0.029	0.866	2.102	0.147
CO ₂ *N	1	5.723	0.017	22.542	<0.001	7.619	0.006	2.999	0.083
I*N	1	43.381	<0.001	11.137	0.001	5.022	0.025	75.769	<0.001
CO ₂ *I*N	1	0.489	0.484	0.041	0.839	0.208	0.649	2.144	0.143

375 *Significance determined using Type II Wald χ^2 tests ($\alpha=0.05$). *P*-values less than 0.05 are in bold. A superscript “a” is included after
 376 trait labels to indicate if models were fit with natural log-transformed response variables. Key: df=degrees of freedom, χ^2 =Wald chi-
 377 square test statistic, *N_{area}*=leaf nitrogen content per unit leaf area (gN m⁻²), *N_{mass}*=leaf nitrogen content (gN g⁻¹), *M_{area}*=leaf mass per
 378 unit leaf area (g m⁻²).

379

380 **Figure 1**

381
382 **Figure 1** Effects of CO₂ concentration, nitrogen fertilization, and inoculation on leaf nitrogen per
383 unit leaf area (a), leaf nitrogen per unit leaf mass (b), leaf mass per unit leaf area (c), and
384 chlorophyll content per unit leaf area (d). Nitrogen fertilization is represented on the x-axis in all
385 panels. Red shaded points and trendlines indicate plants grown under eCO₂, while blue shaded
386 points and trendlines indicate plants grown under aCO₂. Light blue and red circular points and
387 trendlines indicate measurements collected from uninoculated plants, while dark blue and red
388 triangular points indicate measurements collected from inoculated plants. Solid trendlines
389 indicate regression slopes that are different from zero ($p < 0.05$), while dashed trendlines indicate
390 slopes that are not distinguishable from zero ($p > 0.05$).
391

392 *Gas exchange*
393 eCO₂ decreased $A_{\text{net},420}$ by 17% ($p<0.001$; Table 2) and increased $A_{\text{net,growth}}$ by 33% ($p<0.001$;
394 Table 2). Nitrogen fertilization did not modify effects of eCO₂ on $A_{\text{net},420}$ or $A_{\text{net,growth}}$ (CO₂-by-
395 nitrogen fertilization interaction: $p>0.05$ in both cases; Table 2; Fig. 2a-b). Inoculation did not
396 modify $A_{\text{net},420}$ responses to eCO₂ (CO₂-by-inoculation interaction: $p>0.05$). However, an
397 interaction between CO₂ and inoculation ($p<0.05$; Table 2) indicated that inoculated plants
398 experienced a stronger increase in $A_{\text{net,growth}}$ due to eCO₂ (38% increase; Tukey test of the CO₂
399 effect in inoculated plants: $p<0.001$) compared to uninoculated plants (26% increase; Tukey test
400 of the CO₂ effect in uninoculated plants: $p<0.05$). An interaction between nitrogen fertilization
401 and inoculation ($p<0.001$ in both cases; Table 2) indicated that positive effects of increasing
402 nitrogen fertilization on $A_{\text{net},420}$ and $A_{\text{net,growth}}$ ($p<0.001$ in both cases; Table 2; Fig. 2a-b) were
403 stronger in uninoculated plants than inoculated plants (Tukey test comparing the nitrogen
404 fertilization-trait slope between inoculation treatments: $p<0.001$ in both cases).

405 eCO₂ decreased $V_{\text{cmax}25}$ and $J_{\text{max}25}$ by 16% and 10%, respectively, increasing
406 $J_{\text{max}25}:V_{\text{cmax}25}$ by 8% ($p<0.05$ in all cases; Table 2; Fig. 2c-e). $V_{\text{cmax}25}$, $J_{\text{max}25}$, and $J_{\text{max}25}:V_{\text{cmax}25}$
407 responses to eCO₂ were not modified by nitrogen fertilization (CO₂-by-nitrogen fertilization
408 interaction: $p>0.05$ in all cases; Table 2; Fig. 2c-e) or inoculation (CO₂-by-inoculation
409 interaction: $p>0.05$ in all cases; Table 2). An interaction between nitrogen fertilization and
410 inoculation ($p<0.05$ in both cases; Table 2) indicated that positive effects of increasing nitrogen
411 fertilization on $V_{\text{cmax}25}$ and $J_{\text{max}25}$ ($p<0.001$ in both cases; Table 2) and negative effects of
412 increasing nitrogen fertilization on $J_{\text{max}25}:V_{\text{cmax}25}$ ($p<0.001$; Table 2) were driven by uninoculated
413 plants (Tukey test of the nitrogen fertilization-trait slope in uninoculated plants: $p<0.001$ in all
414 cases), as there was no effect of nitrogen fertilization on $V_{\text{cmax}25}$, $J_{\text{max}25}$, or $J_{\text{max}25}:V_{\text{cmax}25}$ in
415 inoculated plants (Tukey test of the nitrogen fertilization-trait slope in inoculated plants: $p>0.05$
416 in all cases).

417 There was no effect of CO₂ concentration on $R_{\text{d}25}$ ($p>0.05$; Table 2). An interaction
418 between nitrogen fertilization and inoculation ($p<0.001$; Table 2) indicated that the positive
419 effect of increasing nitrogen fertilization on $R_{\text{d}25}$ ($p<0.05$; Table 2) was driven by uninoculated
420 plants (Tukey test of the nitrogen fertilization- $R_{\text{d}25}$ slope in uninoculated plants: $p<0.001$), as
421 there was no effect of nitrogen fertilization on $R_{\text{d}25}$ in inoculated plants (Tukey test of the
422 nitrogen fertilization- $R_{\text{d}25}$ slope in inoculated plants: $p>0.05$).

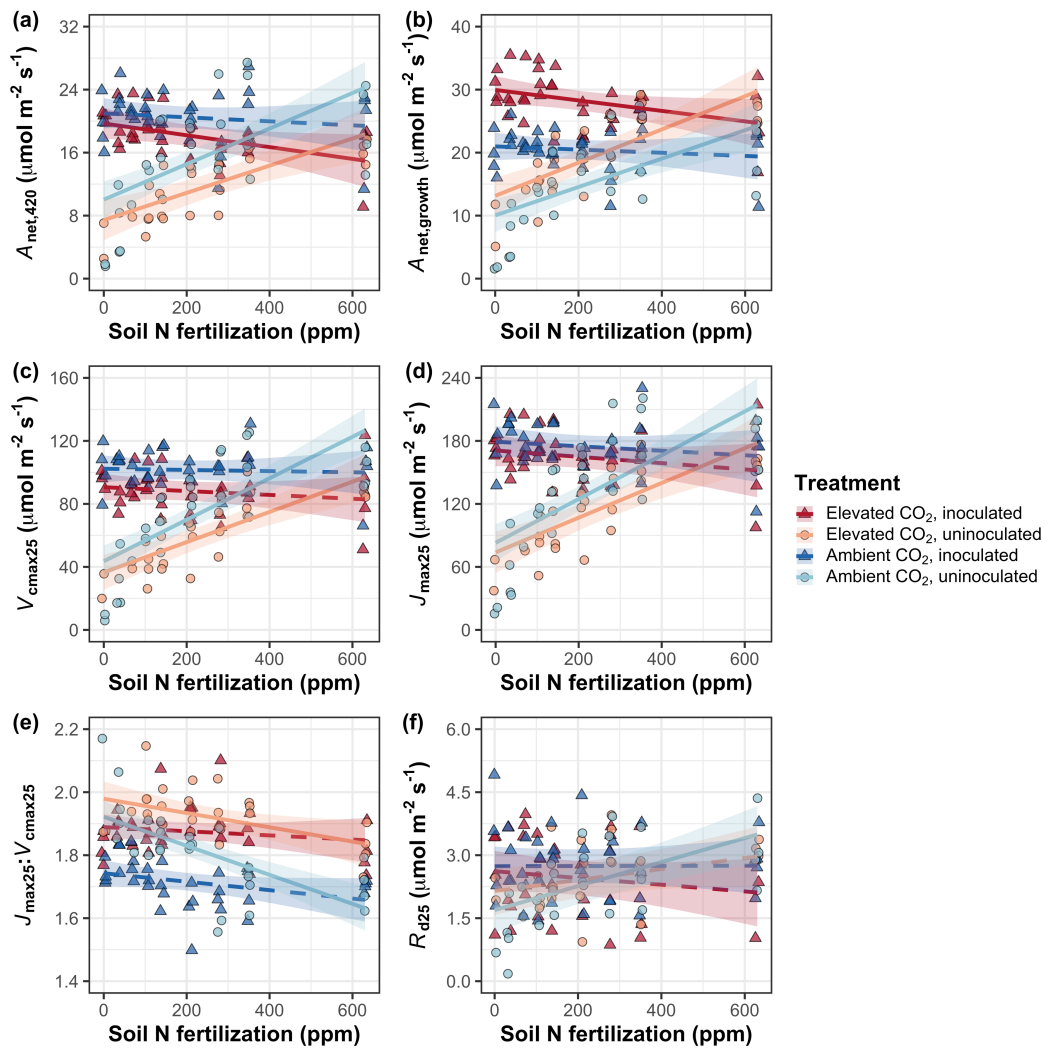
423

Table 2 Effects of CO₂ concentration, inoculation, and nitrogen fertilization on leaf gas exchange*

		<i>A</i> _{net,420}		<i>A</i> _{net,growth}		<i>V</i> _{cmax25}		<i>J</i> _{max25}	
	df	χ^2	p	χ^2	p	χ^2	p	χ^2	p
CO ₂	1	15.747	<0.001	52.716	<0.001	18.039	<0.001	6.042	0.014
Inoculation (I)	1	77.137	<0.001	83.008	<0.001	98.579	<0.001	85.064	<0.001
N fertilization (N)	1	11.986	<0.001	14.658	<0.001	37.053	<0.001	25.356	<0.001
CO ₂ *I	1	1.032	0.310	5.634	0.018	0.065	0.799	0.667	0.414
CO ₂ *N	1	1.998	0.158	0.135	0.713	1.758	0.185	0.742	0.389
I*N	1	46.800	<0.001	50.774	<0.001	60.394	<0.001	57.41	<0.001
CO ₂ *I*N	1	0.002	0.964	1.332	0.248	0.748	0.387	0.377	0.539

	<i>J</i> _{max25:<i>V</i>_{cmax25}}		<i>R</i> _{d25}		
	χ^2	p	χ^2	p	
CO ₂	1	92.010	<0.001	0.256	0.613
Inoculation (I)	1	27.768	<0.001	3.094	0.079
N fertilization (N)	1	28.147	<0.001	5.965	0.015
CO ₂ *I	1	2.916	0.088	2.563	0.109
CO ₂ *N	1	3.210	0.073	2.675	0.102
I*N	1	9.607	0.002	12.083	0.001
CO ₂ *I*N	1	1.102	0.294	0.244	0.622

424 *Significance determined using Type II Wald χ^2 tests ($\alpha=0.05$). P-values less than 0.05 are in bold. Key: df=degrees of freedom,425 χ^2 =Wald chi-square test statistic, A_{net} =net photosynthesis rate ($\mu\text{mol m}^{-2} \text{s}^{-1}$), V_{cmax25} =maximum rate of Rubisco carboxylation at 25°C426 ($\mu\text{mol m}^{-2} \text{s}^{-1}$), J_{max25} =maximum rate of electron transport for RuBP regeneration at 25°C ($\mu\text{mol m}^{-2} \text{s}^{-1}$), $J_{max25}:V_{cmax25}$ =ratio of J_{max25} 427 to V_{cmax25} (unitless), R_{d25} =dark respiration at 25°C ($\mu\text{mol m}^{-2} \text{s}^{-1}$)

428 **Figure 2**

429

430 **Figure 2** Effects of CO₂, nitrogen fertilization, and inoculation on net photosynthesis measured
 431 at 420 $\mu\text{mol mol}^{-1}$ CO₂ (a), net photosynthesis measured under growth CO₂ concentration (b), the
 432 maximum rate of Rubisco carboxylation at 25°C (c), the maximum rate of electron transport for
 433 RuBP regeneration at 25°C (d), the ratio of the maximum rate of electron transport for RuBP
 434 regeneration to the maximum rate of Rubisco carboxylation (e), and dark respiration at 25°C (f).
 435 Nitrogen fertilization is represented on the x-axis. Red shaded points and trendlines indicate
 436 plants grown under eCO₂, while blue shaded points and trendlines indicate plants grown under
 437 aCO₂. Light blue and red circular points and trendlines indicate measurements collected from
 438 uninoculated plants, while dark blue and red triangular points indicate measurements collected
 439 from inoculated plants. Solid trendlines indicate regression slopes that are different from zero
 440 ($p < 0.05$), while dashed trendlines indicate slopes that are not distinguishable from zero ($p > 0.05$).

441 *Whole-plant traits*
442 eCO₂ increased total leaf area and total biomass by 51% and 102%, respectively ($p<0.001$ in
443 both cases; Table 3). Positive effects of eCO₂ on total leaf area and total biomass were enhanced
444 with increasing nitrogen fertilization (CO₂-by-nitrogen fertilization interaction: $p<0.001$ in both
445 cases; Table 3; Fig. 4a-b) but not inoculation (CO₂-by-inoculation interaction: $p>0.05$ in both
446 cases; Table 3). An interaction between nitrogen fertilization and inoculation ($p<0.001$ in both
447 cases; Table 3) indicated that the positive effects of increasing nitrogen fertilization on total leaf
448 area and total biomass ($p<0.001$ in both cases; Table 3) were stronger in uninoculated plants than
449 inoculated plants (Tukey tests comparing the nitrogen fertilization-trait slopes between
450 inoculation treatments: $p<0.05$ for both traits).

451 eCO₂ increased N_{cost} by 62% ($p<0.001$; Table 3), a pattern that was not modified by
452 nitrogen fertilization (CO₂-by-nitrogen fertilization interaction: $p>0.05$; Table 3). An interaction
453 between CO₂ and inoculation ($p<0.05$; Table 3) indicated that the positive effect of eCO₂ on N_{cost}
454 was stronger in uninoculated plants (99% increase; Tukey test evaluating the CO₂ effect on N_{cost}
455 in uninoculated plants: $p<0.001$) than inoculated plants (21% increase Tukey test evaluating the
456 CO₂ effect on N_{cost} in inoculated plants: $p<0.05$). An interaction between nitrogen fertilization
457 and inoculation ($p<0.001$; Table 3) indicated that the negative effect of increasing nitrogen
458 fertilization on N_{cost} ($p<0.001$; Table 3) was stronger in uninoculated plants (Tukey test
459 comparing the nitrogen fertilization- N_{cost} slope between inoculation treatments: $p<0.001$). A
460 three-way interaction ($p<0.001$; Table 3) indicated that interactions between nitrogen fertilization
461 and inoculation were stronger under eCO₂ than aCO₂. This pattern was driven by greater N_{cost} in
462 uninoculated plants grown under eCO₂ and low nitrogen fertilization than any other CO₂-by-
463 inoculation treatment combination under low nitrogen fertilization (Tukey test comparing N_{cost} in
464 uninoculated individuals grown under eCO₂ and 0 ppm N to all other CO₂-inoculation treatment
465 combinations grown under 0 ppm N: $p<0.001$ in all cases; Fig. 4c).

466

467 *Nitrogen fixation*

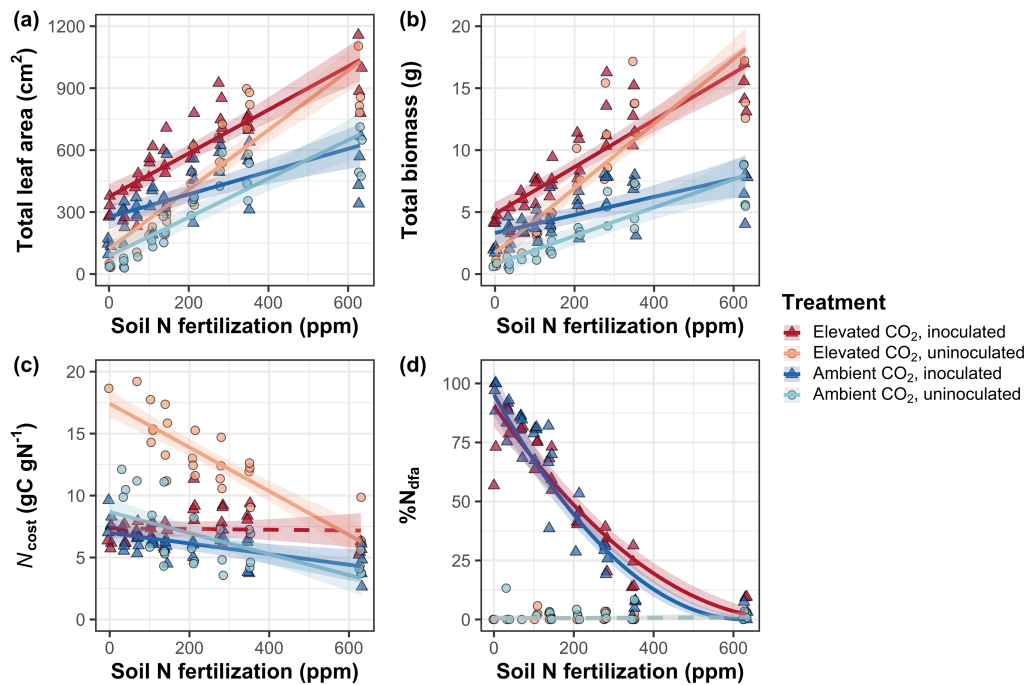
468 There was no CO₂ effect on % N_{dfa} ($p=0.472$; Table 3; Fig. 4d). An interaction between nitrogen
469 fertilization and inoculation ($p<0.001$; Table 3) indicated that the negative effect of increasing
470 nitrogen fertilization on % N_{dfa} ($p<0.001$; Table 3) was driven by inoculated plants (Tukey test of
471 the nitrogen fertilization-% N_{dfa} slope in inoculated plants: $p<0.001$), as there was no effect of

472 nitrogen fertilization on $\%N_{dfa}$ in uninoculated plants (Tukey test of the nitrogen fertilization-
473 $\%N_{dfa}$ slope in uninoculated plants: $p>0.05$; Fig. 4d).
474

475 **Table 3** Effects of CO₂ concentration, inoculation, and nitrogen fertilization on whole-plant growth, carbon costs to acquire nitrogen,
 476 and investment toward symbiotic nitrogen fixation*

		Total leaf area		Total biomass ^b		Carbon cost to acquire nitrogen		%N _{dfa} ^b	
	df	χ^2	p	χ^2	p	χ^2	p	χ^2	p
CO ₂	1	69.291	<0.001	131.477	<0.001	88.189	<0.001	0.518	0.472
Inoculation (I)	1	35.715	<0.001	34.264	<0.001	136.343	<0.001	955.57	<0.001
N fertilization (N)	1	274.199	<0.001	269.046	<0.001	80.501	<0.001	292.938	<0.001
CO ₂ *I	1	2.064	0.151	0.518	0.472	85.237	<0.001	2.010	0.156
CO ₂ *N	1	18.655	<0.001	16.877	<0.001	1.050	0.306	2.716	0.099
I*N	1	10.804	0.001	15.779	<0.001	46.489	<0.001	231.29	<0.001
CO ₂ *I*N	1	<0.001	0.990	0.023	0.880	18.125	<0.001	2.119	0.145

477 *Significance determined using Type II Wald χ^2 tests ($\alpha=0.05$). P-values less than 0.05 are in bold. A superscript “^b” after trait labels
 478 indicates if models were fit using square root transformed variables. Key: df=degrees of freedom, χ^2 =Wald chi-square test statistic,
 479 total leaf area (cm²), total biomass (g), carbon cost to acquire nitrogen (gC gN⁻¹), %N_{dfa}=percent leaf nitrogen content fixed from the
 480 atmosphere (%).

482 **Figure 3**

483

484 **Figure 3.** Effects of CO₂, nitrogen fertilization, and inoculation on total leaf area (a), total
 485 biomass (b), structural carbon costs to acquire nitrogen (c), and percent of leaf nitrogen content
 486 derived from the atmosphere (d). Nitrogen fertilization is represented on the x-axis. Red shaded
 487 points and trendlines indicate plants grown under eCO₂, while blue shaded points and trendlines
 488 indicate plants grown under aCO₂. Light blue and red circular points and trendlines indicate
 489 measurements collected from uninoculated plants, while dark blue and red triangular points
 490 indicate measurements collected from inoculated plants. Solid trendlines indicate regression
 491 slopes that are different from zero ($p < 0.05$), while dashed trendlines indicate slopes that are not
 492 distinguishable from zero ($p > 0.05$).
 493

494 **Discussion**

495 *Glycine max* seedlings were grown under two CO₂ concentrations, two inoculation treatments,
496 and nine nitrogen fertilization treatments in a full-factorial growth chamber experiment to
497 reconcile the role of nitrogen availability, demand, and acquisition strategy on leaf and whole-
498 plant responses to eCO₂. eCO₂ increased $A_{\text{net,growth}}$ despite reduced N_{area} , V_{cmax25} , and J_{max25} .
499 Larger reductions in V_{cmax25} than J_{max25} increased $J_{\text{max25}}:V_{\text{cmax25}}$, while respective increases and
500 decreases in $A_{\text{net,growth}}$ and N_{area} increased photosynthetic nitrogen-use efficiency. These patterns
501 are consistent with previous studies that have investigated or reviewed leaf responses to eCO₂
502 (Drake *et al.*, 1997; Ainsworth *et al.*, 2002; Ainsworth & Long, 2005; Ainsworth & Rogers,
503 2007; Crous *et al.*, 2010; Lee *et al.*, 2011; Smith & Dukes, 2013; Poorter *et al.*, 2022). Positive
504 effects of eCO₂ on $A_{\text{net,growth}}$ and $J_{\text{max25}}:V_{\text{cmax25}}$ and negative effects of eCO₂ on V_{cmax25} and J_{max25}
505 were not related to nitrogen availability, following patterns expected from eco-evolutionary
506 optimality theory (Smith & Keenan, 2020; Harrison *et al.*, 2021; Dong *et al.*, 2022b). In further
507 support of the theory, increased $J_{\text{max25}}:V_{\text{cmax25}}$ and photosynthetic nitrogen-use efficiency provide
508 strong support for the idea that leaves were downregulating V_{cmax25} in response to eCO₂ such that
509 enhanced net photosynthesis rates approached optimal coordination of Rubisco carboxylation
510 and electron transport for RuBP regeneration (Chen *et al.*, 1993; Maire *et al.*, 2012; Smith &
511 Keenan, 2020), decreasing demand for building and maintaining photosynthetic enzymes (Dong
512 *et al.*, 2022b).

513 Leaf photosynthetic responses to eCO₂ corresponded with increased total leaf area and
514 total biomass, patterns that are also consistent with previous studies that have investigated or
515 reviewed whole-plant responses to eCO₂ (Ainsworth *et al.*, 2002; Ainsworth & Long, 2005;
516 Smith & Dukes, 2013; Poorter *et al.*, 2022). Greater whole-plant growth under eCO₂ was
517 associated with greater carbon costs to acquire nitrogen through stronger increases in
518 belowground carbon allocation than whole-plant nitrogen uptake, indicating that plants grown
519 under eCO₂ supported greater total leaf area and total biomass through increased plant nitrogen
520 uptake, though at reduced nitrogen uptake efficiency. Unlike leaf photosynthetic responses,
521 increasing nitrogen fertilization enhanced positive whole-plant responses to eCO₂, supporting
522 our hypothesis that nitrogen availability would constrain whole-plant responses to eCO₂. Positive
523 effects of increasing nitrogen fertilization on total leaf area and total biomass were associated
524 with reductions in carbon costs to acquire nitrogen, a pattern driven by stronger increases in

whole-plant nitrogen uptake than belowground carbon allocation (Perkowski *et al.*, 2021). While reductions in carbon costs to acquire nitrogen due to increasing nitrogen fertilization were similar between CO₂ treatments, increasing nitrogen fertilization increased whole-plant nitrogen uptake more strongly under eCO₂. This pattern, coupled with similar effects of nitrogen fertilization on belowground carbon allocation responses to eCO₂, indicated that increasing fertilization enhanced positive growth responses to eCO₂ through increased nitrogen uptake efficiency. These findings support previous results suggesting that positive effects of nitrogen availability on whole-plant responses to eCO₂ are linked to reduced costs of acquiring nitrogen and increased nitrogen uptake efficiency (Terrer *et al.*, 2018).

Nitrogen availability and demand could each explain plant responses to eCO₂, though these factors operated at different levels of organization. Specifically, eCO₂ increased net photosynthesis rates through increasingly optimal coordination of Rubisco carboxylation and electron transport for RuBP regeneration (Chen *et al.*, 1993; Maire *et al.*, 2012), a pattern that reduced leaf nitrogen demand for building and maintaining photosynthetic enzymes and was independent of changes in nitrogen fertilization. Nitrogen availability enhanced whole-plant responses to eCO₂ despite no apparent effect of nitrogen fertilization at the leaf level. Interestingly, optimized nitrogen allocation to photosynthetic capacity may have resulted in nitrogen savings at the leaf level that could have maximized nitrogen allocation to growth. These results suggest that plants grown under eCO₂ responded to increased nitrogen availability by increasing the number of optimally coordinated leaves and that the downregulation in photosynthetic capacity under eCO₂ was not a direct response to changes in nitrogen availability.

547 Inoculation does not affect leaf or whole-plant responses to eCO₂

Inoculation increased N_{area} , $A_{\text{net},420}$, $A_{\text{net,growth}}$, $V_{\text{cmax}25}$, $J_{\text{max}25}$, total leaf area, and total biomass, and decreased $J_{\text{max}25}:V_{\text{cmax}25}$ and $R_{\text{d}25}$. These patterns support previous literature suggesting that species that form associations with symbiotic nitrogen-fixing bacteria have increased leaf nitrogen content, photosynthetic capacity, and growth compared to species that do not form such associations (Adams *et al.*, 2016; Bytnerowicz *et al.*, 2023). Positive effects of inoculation on leaf and whole-plant traits were most apparent under low nitrogen fertilization and rapidly diminished with increasing nitrogen fertilization as plant investment in symbiotic nitrogen fixation decreased, supporting the idea that nitrogen fixation is a nutrient acquisition strategy that

556 may confer competitive benefits for nitrogen-fixing species growing in low soil nitrogen
557 environments (Rastetter *et al.*, 2001; Andrews *et al.*, 2011; McCulloch & Porder, 2021).

558 Interestingly, inoculation did not modify the effect of eCO₂ on V_{cmax25} , J_{max25} ,
559 J_{max25} : V_{cmax25} , total leaf area, or total biomass. These patterns corresponded with null effects of
560 eCO₂ on %N_{dfa} and the ratio of root nodule biomass to root biomass, suggesting that null
561 inoculation effects on plant responses to eCO₂ were due to similar plant investments toward
562 symbiotic nitrogen fixation between CO₂ treatments. We observed these patterns regardless of
563 nitrogen fertilization level, contrasting our hypothesis that inoculation would enhance whole-
564 plant responses to eCO₂ under low nitrogen fertilization, where individuals invested more
565 strongly in symbiotic nitrogen fixation. These patterns also contrast previous work showing that
566 plant investment toward symbiotic nitrogen fixation tends to be greater under scenarios that
567 increase whole-plant demand to acquire nitrogen (Taylor & Menge, 2018; Friel & Friesen, 2019;
568 McCulloch & Porder, 2021; Perkowski *et al.*, 2021). Interestingly, stronger positive effects of
569 eCO₂ on $A_{net,growth}$ in inoculated individuals support previously work (Ainsworth *et al.*, 2002).
570 However, this response was not due to alterations in plant investment toward the symbiosis.
571

572 *Modeling implications*

573 Many terrestrial biosphere models predict photosynthetic capacity through parameterized
574 relationships between N_{area} and V_{cmax} (Smith & Dukes, 2013; Rogers *et al.*, 2017), which assumes
575 that leaf nitrogen-photosynthesis relationships are constant across growing environments. Our
576 results build on previous work suggesting that leaf nitrogen-photosynthesis relationships
577 dynamically change across growing environments (Luo *et al.*, 2021; Waring *et al.*, 2023), as
578 eCO₂ reduced leaf nitrogen content more strongly than it increased $A_{net,growth}$ and decreased
579 V_{cmax25} and J_{max25} . Additionally, the positive effect of increasing nitrogen fertilization on indices
580 of photosynthetic capacity was only apparent in uninoculated plants, as nitrogen fertilization did
581 not affect V_{cmax25} or J_{max25} in inoculated plants. The positive effect of increasing nitrogen
582 fertilization on N_{area} and Chl_{area} was also markedly weaker in inoculated plants than in
583 uninoculated plants. These patterns indicate that leaf nitrogen-photosynthesis relationships are
584 context-dependent on nitrogen acquisition strategy, may only be constant in environments where
585 nitrogen availability limits leaf physiology, and will likely shift in response to increasing
586 atmospheric CO₂ concentrations. Terrestrial biosphere models that predict photosynthetic

587 capacity through parameterized relationships between N_{area} and V_{cmax} (Kattge *et al.*, 2009;
588 Walker *et al.*, 2014) may risk overestimating photosynthetic capacity, therefore net primary
589 productivity and the magnitude of the land carbon sink, under future novel growth environments.

590 Our results demonstrate that optimal resource allocation to photosynthetic capacity
591 defines leaf photosynthetic responses to eCO₂ and that these responses are independent of
592 nitrogen availability. Current approaches for simulating photosynthetic responses to CO₂ in
593 terrestrial biosphere models with coupled carbon and nitrogen cycles often invoke patterns
594 expected from progressive nitrogen limitation, where photosynthetic responses to eCO₂ are
595 modeled as a function of positive relationships between nitrogen availability and leaf nitrogen
596 content (Smith & Dukes, 2013; Wieder *et al.*, 2015; Rogers *et al.*, 2017). Findings presented here
597 contradict this framework, suggesting that leaf photosynthetic responses to eCO₂ result in
598 optimized nitrogen allocation to satisfy reduced leaf nitrogen demand to build and maintain
599 photosynthetic enzymes. Optimality models that use principles from optimal coordination and
600 photosynthetic least-cost theories are capable of capturing photosynthetic responses to CO₂
601 independent of nitrogen availability (Smith & Keenan, 2020; Harrison *et al.*, 2021), suggesting
602 that including optimality frameworks in terrestrial biosphere models may improve the accuracy
603 by which models simulate photosynthetic processes in response to increasing atmospheric CO₂
604 concentrations.

605 Previous work has highlighted that pot experiments restrict belowground rooting volume
606 and may alter plant allocation responses to environmental change (Ainsworth *et al.*, 2002;
607 Poorter *et al.*, 2012). In this study, the ratio of pot volume to total biomass was greater under
608 eCO₂ and increased with increasing nitrogen fertilization such that several treatment
609 combinations exceeded values recommended to avoid growth limitation imposed by pot volume
610 (<1 g L⁻¹; Table S6; Fig. S6) (Poorter *et al.*, 2012). However, there was no evidence to suggest
611 that pot size limited plant growth, as evidenced by the lack of a saturating effect of increasing
612 fertilization on total biomass, belowground carbon biomass, or root biomass under conditions
613 where biomass: pot volume ratios exceeded 1 g L⁻¹ (e.g., individuals of either inoculation status
614 grown under high fertilization and eCO₂). Field studies that do not restrict belowground rooting
615 volume observed similar leaf and whole-plant responses to eCO₂ (Crous *et al.*, 2010; Lee *et al.*,
616 2011; Pastore *et al.*, 2019; Smith & Keenan, 2020), indicating that the pot volume used in this
617 study (6 L) was likely sufficient to avoid growth limitation.

618

619 *Conclusions*

620 Nitrogen availability and demand for building and maintaining photosynthetic enzymes each
621 helped explain *G. max* responses to eCO₂, though operated at different scales. Supporting eco-
622 evolutionary optimality theory, leaf photosynthetic responses to eCO₂ were independent of
623 nitrogen availability and, in most cases, inoculation. Instead, eCO₂ decreased the maximum rate
624 of Rubisco carboxylation more strongly than it decreased the maximum rate of electron transport
625 for RuBP regeneration, allowing increased net photosynthesis rates to approach optimal
626 coordination while reducing leaf nitrogen demand to build and maintain photosynthetic enzymes.
627 Supporting the progressive nitrogen limitation hypothesis, nitrogen availability enhanced whole-
628 plant responses to eCO₂ due to increased plant nitrogen uptake and reduced costs of nitrogen
629 acquisition. Additionally, cascading effects of nitrogen savings at the leaf level may have
630 maximized nitrogen allocation to whole-plant growth. Inoculation did not modify whole-plant
631 responses to eCO₂ due to similar plant investment toward symbiotic nitrogen fixation between
632 CO₂ treatments. Overall, results indicate that plants grown under eCO₂ responded to increased
633 nitrogen availability by increasing the number of optimally coordinated leaves, and changes in
634 nitrogen availability did not modify the downregulation in photosynthetic capacity under eCO₂.
635 The differential role of nitrogen availability on leaf and whole-plant responses to eCO₂ coupled
636 with dynamic leaf nitrogen-photosynthesis relationships across CO₂ and nitrogen fertilization
637 treatments suggests that terrestrial biosphere models may improve simulations of photosynthetic
638 responses to increasing atmospheric CO₂ concentrations by adopting frameworks that include
639 optimality principles.

640

641 **Conflicts of Interest**

642 The authors declare no conflicts of interest.

643

644 **Acknowledgements**

645 This study is a contribution to the LEMONTREE (Land Ecosystem Models based On New
646 Theory, obseRvations and ExperimEnts) project, funded through the generosity of Eric and
647 Wendy Schmidt by recommendation of the Schmidt Futures programme. EAP acknowledges
648 support from a Texas Tech University Doctoral Dissertation Completion Fellowship and a

649 Botanical Society of America Graduate Student Research Award. This work was also supported
650 by US National Science Foundation awards to NGS (DEB-2045968 and DEB-2217353).

651

652 Data Availability

653 All R scripts, data, and metadata are available at <https://doi.org/10.5281/zenodo.10177575> (or on
654 GitHub at: https://github.com/eaperkowski/NxCO2xI_ms_data)

655

656 Author contributions

657 EAP conceptualized the study objectives and designed the experiment in collaboration with
658 NGS, collected data, conducted data analysis, and wrote the first manuscript draft. EE assisted
659 with data collection and experiment maintenance. NGS conceptualized study objectives and
660 experimental design with EAP and oversaw experiment progress. All authors provided
661 manuscript feedback and approved the manuscript in its current form for submission to *New
662 Phytologist*.

663

664 References

- 665 **Adams MA, Turnbull TL, Sprent JI, Buchmann N.** 2016. Legumes are different: Leaf
666 nitrogen, photosynthesis, and water use efficiency. *Proceedings of the National Academy of
667 Sciences of the United States of America* **113**: 4098–4103.
- 668 **Ainsworth EA, Davey PA, Bernacchi CJ, Dermody OC, Heaton EA, Moore DJ, Morgan
669 PB, Naidu SL, Ra HSY, Zhu XG, et al.** 2002. A meta-analysis of elevated [CO₂] effects on
670 soybean (*Glycine max*) physiology, growth and yield. *Global Change Biology* **8**: 695–709.
- 671 **Ainsworth EA, Long SP.** 2005. What have we learned from 15 years of free-air CO₂ enrichment
672 (FACE)? A meta-analytic review of the responses of photosynthesis, canopy properties and plant
673 production to rising CO₂. *New Phytologist* **165**: 351–372.
- 674 **Ainsworth EA, Rogers A.** 2007. The response of photosynthesis and stomatal conductance to
675 rising [CO₂]: mechanisms and environmental interactions. *Plant, Cell & Environment* **30**: 258–
676 270.
- 677 **Andrews M, James EK, Sprent JI, Boddey RM, Gross E, dos Reis FB.** 2011. Nitrogen
678 fixation in legumes and actinorhizal plants in natural ecosystems: Values obtained using ¹⁵N
679 natural abundance. *Plant Ecology and Diversity* **4**: 117–130.
- 680 **Arora VK, Katavouta A, Williams RG, Jones CD, Brovkin V, Friedlingstein P, Schwinger
681 J, Bopp L, Boucher O, Cadule P, et al.** 2020. Carbon-concentration and carbon-climate
682 feedbacks in CMIP6 models and their comparison to CMIP5 models. *Biogeosciences* **17**: 4173–
683 4222.
- 684 **Barnes JD, Balaguer L, Manrique E, Elvira S, Davison AW.** 1992. A reappraisal of the use of
685 DMSO for the extraction and determination of chlorophylls a and b in lichens and higher plants.
686 *Environmental and Experimental Botany* **32**: 85–100.

- 687 **Bates D, Mächler M, Bolker B, Walker S.** 2015. Fitting linear mixed-effects models using
688 lme4. *Journal of Statistical Software* **67**: 1–48.
- 689 **Bernacchi CJ, Singsaas EL, Pimentel C, Portis AR, Long SP.** 2001. Improved temperature
690 response functions for models of Rubisco-limited photosynthesis. *Plant, Cell and Environment*
691 **24**: 253–259.
- 692 **Brzostek ER, Fisher JB, Phillips RP.** 2014. Modeling the carbon cost of plant nitrogen
693 acquisition: Mycorrhizal trade-offs and multipath resistance uptake improve predictions of
694 retranslocation. *Journal of Geophysical Research: Biogeosciences* **119**: 1684–1697.
- 695 **Bytnerowicz TA, Funk JL, Menge DNL, Perakis SS, Wolf AA.** 2023. Leaf nitrogen affects
696 photosynthesis and water use efficiency similarly in nitrogen-fixing and non-fixing trees. *Journal*
697 *of Ecology*: 1–15.
- 698 **Chen J-L, Reynolds JF, Harley PC, Tenhunen JD.** 1993. Coordination theory of leaf nitrogen
699 distribution in a canopy. *Oecologia* **93**: 63–69.
- 700 **Crous KY, Reich PB, Hunter MD, Ellsworth DS.** 2010. Maintenance of leaf N controls the
701 photosynthetic CO₂ response of grassland species exposed to 9 years of free-air CO₂ enrichment.
702 *Global Change Biology* **16**: 2076–2088.
- 703 **Curtis PS.** 1996. A meta-analysis of leaf gas exchange and nitrogen in trees grown under
704 elevated carbon dioxide. *Plant, Cell and Environment* **19**: 127–137.
- 705 **Davies-Barnard T, Meyerholt J, Zaeble S, Friedlingstein P, Brovkin V, Fan Y, Fisher RA,**
706 **Jones CD, Lee H, Peano D, et al.** 2020. Nitrogen cycling in CMIP6 land surface models:
707 progress and limitations. *Biogeosciences* **17**: 5129–5148.
- 708 **Dong N, Prentice IC, Evans BJ, Caddy-Retalic S, Lowe AJ, Wright IJ.** 2017. Leaf nitrogen
709 from first principles: field evidence for adaptive variation with climate. *Biogeosciences* **14**: 481–
710 495.
- 711 **Dong N, Prentice IC, Wright IJ, Evans BJ, Togashi HF, Caddy-Retalic S, McInerney FA,**
712 **Sparrow B, Leitch E, Lowe AJ.** 2020. Components of leaf-trait variation along environmental
713 gradients. *New Phytologist* **228**: 82–94.
- 714 **Dong N, Prentice IC, Wright IJ, Wang H, Atkin OK, Bloomfield KJ, Domingues TF,**
715 **Gleason SM, Maire V, Onoda Y, et al.** 2022a. Leaf nitrogen from the perspective of optimal
716 plant function. *Journal of Ecology* **110**: 2585–2602.
- 717 **Dong N, Wright IJ, Chen JM, Luo X, Wang H, Keenan TF, Smith NG, Prentice IC.** 2022b.
718 Rising CO₂ and warming reduce global canopy demand for nitrogen. *New Phytologist* **235**:
719 1692–1700.
- 720 **Drake BG, González-Meler MA, Long SP.** 1997. More efficient plants: a consequence of
721 rising atmospheric CO₂? *Annual Review of Plant Biology* **48**: 609–639.
- 722 **Duursma RA.** 2015. Plantcophys - an R package for analysing and modelling leaf gas
723 exchange data. *PLOS ONE* **10**: e0143346.
- 724 **Evans JR.** 1989. Photosynthesis and nitrogen relationships in leaves of C₃ plants. *Oecologia* **78**:
725 9–19.
- 726 **Evans JR, Clarke VC.** 2019. The nitrogen cost of photosynthesis. *Journal of Experimental*
727 *Botany* **70**: 7–15.
- 728 **Farquhar GD, von Caemmerer S, Berry JA.** 1980. A biochemical model of photosynthetic
729 CO₂ assimilation in leaves of C₃ species. *Planta* **149**: 78–90.
- 730 **Field CB, Mooney HA.** 1986. The photosynthesis-nitrogen relationship in wild plants. In:
731 Givnish TJ, ed. *On the Economy of Plant Form and Function*. Cambridge: Cambridge University
732 Press, 25–55.

- 733 **Finzi AC, Moore DJP, DeLucia EH, Lichter J, Hofmockel KS, Jackson RB, Kim HS,**
734 **Matamala R, McCarthy HR, Oren R, et al.** 2006. Progressive nitrogen limitation of ecosystem
735 processes under elevated CO₂ in a warm-temperate forest. *Ecology* **87**: 15–25.
- 736 **Fox J, Weisberg S.** 2019. *An R companion to applied regression*. Thousand Oaks, California:
737 Sage.
- 738 **Friedlingstein P, Meinshausen M, Arora VK, Jones CD, Anav A, Liddicoat SK, Knutti R.**
739 2014. Uncertainties in CMIP5 climate projections due to carbon cycle feedbacks. *Journal of*
740 *Climate* **27**: 511–526.
- 741 **Friel CA, Friesen ML.** 2019. Legumes modulate allocation to rhizobial nitrogen fixation in
742 response to factorial light and nitrogen manipulation. *Frontiers in Plant Science* **10**: 1316.
- 743 **Harrison SP, Cramer W, Franklin O, Prentice IC, Wang H, Bränström Å, de Boer H,**
744 **Dieckmann U, Joshi J, Keenan TF, et al.** 2021. Eco-evolutionary optimality as a means to
745 improve vegetation and land-surface models. *New Phytologist* **231**: 2125–2141.
- 746 **Hoagland DR, Arnon DI.** 1950. The water-culture method for growing plants without soil.
747 *California Agricultural Experiment Station*: 347 347: 1–32.
- 748 **Hungate BA, Dukes JS, Shaw MR, Luo Y, Field CB.** 2003. Nitrogen and climate change.
749 *Science* **302**: 1512–1513.
- 750 **Katabuchi M.** 2015. LeafArea: An R package for rapid digital analysis of leaf area. *Ecological*
751 *Research* **30**: 1073–1077.
- 752 **Kattge J, Knorr W, Raddatz T, Wirth C.** 2009. Quantifying photosynthetic capacity and its
753 relationship to leaf nitrogen content for global-scale terrestrial biosphere models. *Global Change*
754 *Biology* **15**: 976–991.
- 755 **Kenward MG, Roger JH.** 1997. Small sample inference for fixed effects from restricted
756 maximum likelihood. *Biometrics* **53**: 983.
- 757 **Kou-Giesbrecht S, Arora VK, Seiler C, Arneth A, Falk S, Jain AK, Joos F, Kennedy D,**
758 **Knauer J, Sitch S, et al.** 2023. Evaluating nitrogen cycling in terrestrial biosphere models: a
759 disconnect between the carbon and nitrogen cycles. *Earth System Dynamics* **14**: 767–795.
- 760 **LeBauer DS, Treseder K.** 2008. Nitrogen limitation of net primary productivity. *Ecology* **89**:
761 371–379.
- 762 **Lee TD, Barrott SH, Reich PB.** 2011. Photosynthetic responses of 13 grassland species across
763 11 years of free-air CO₂ enrichment is modest, consistent and independent of N supply. *Global*
764 *Change Biology* **17**: 2893–2904.
- 765 **Lenth R.** 2019. emmeans: estimated marginal means, aka least-squares means.
- 766 **Liang J, Qi X, Souza L, Luo Y.** 2016. Processes regulating progressive nitrogen limitation
767 under elevated carbon dioxide: a meta-analysis. *Biogeosciences* **13**: 2689–2699.
- 768 **Luo Y, Currie WS, Dukes JS, Finzi AC, Hartwig UA, Hungate BA, McMurtrie RE, Oren**
769 **R, Parton WJ, Pataki DE, et al.** 2004. Progressive nitrogen limitation of ecosystem responses
770 to rising atmospheric carbon dioxide. *BioScience* **54**: 731–739.
- 771 **Luo X, Keenan TF, Chen JM, Croft H, Prentice IC, Smith NG, Walker AP, Wang H, Wang**
772 **R, Xu C, et al.** 2021. Global variation in the fraction of leaf nitrogen allocated to photosynthesis.
773 *Nature Communications* **12**: 4866.
- 774 **Maire V, Martre P, Kattge J, Gastal F, Esser G, Fontaine S, Soussana J-F.** 2012. The
775 coordination of leaf photosynthesis links C and N fluxes in C₃ plant species. *PLoS ONE* **7**:
776 e38345.
- 777 **McCulloch LA, Porder S.** 2021. Light fuels while nitrogen suppresses symbiotic nitrogen
778 fixation hotspots in neotropical canopy gap seedlings. *New Phytologist* **231**: 1734–1745.

- 779 Meyerholt J, Sickel K, Zaehle S. 2020. Ensemble projections elucidate effects of uncertainty in
780 terrestrial nitrogen limitation on future carbon uptake. *Global Change Biology* **26**: 3978–3996.
- 781 Moore DJP, Aref S, Ho RM, Pippen JS, Hamilton JG, De Lucia EH. 2006. Annual basal area
782 increment and growth duration of *Pinus taeda* in response to eight years of free-air carbon
783 dioxide enrichment. *Global Change Biology* **12**: 1367–1377.
- 784 Norby RJ, Warren JM, Iversen CM, Medlyn BE, McMurtrie RE. 2010. CO₂ enhancement
785 of forest productivity constrained by limited nitrogen availability. *Proceedings of the National
786 Academy of Sciences* **107**: 19368–19373.
- 787 Paillassa J, Wright IJ, Prentice IC, Pepin S, Smith NG, Ethier G, Westerband AC,
788 Lamarque LJ, Wang H, Cornwell WK, et al. 2020. When and where soil is important to
789 modify the carbon and water economy of leaves. *New Phytologist* **228**: 121–135.
- 790 Pastore MA, Lee TD, Hobbie SE, Reich PB. 2019. Strong photosynthetic acclimation and
791 enhanced water-use efficiency in grassland functional groups persist over 21 years of CO₂
792 enrichment, independent of nitrogen supply. *Global Change Biology* **25**: 3031–3044.
- 793 Peng Y, Bloomfield KJ, Cernusak LA, Domingues TF, Prentice IC. 2021. Global climate and
794 nutrient controls of photosynthetic capacity. *Communications Biology* **4**: 462.
- 795 Perkowski EA, Waring EF, Smith NG. 2021. Root mass carbon costs to acquire nitrogen are
796 determined by nitrogen and light availability in two species with different nitrogen acquisition
797 strategies. *Journal of Experimental Botany* **72**: 5766–5776.
- 798 Poorter H, Böhler J, Van Dusschoten D, Climent J, Postma JA. 2012. Pot size matters: A
799 meta-analysis of the effects of rooting volume on plant growth. *Functional Plant Biology* **39**:
800 839–850.
- 801 Poorter H, Knopf O, Wright IJ, Temme AA, Hogewoning SW, Graf A, Cernusak LA, Pons
802 TL. 2022. A meta-analysis of responses of C₃ plants to atmospheric CO₂: dose–response curves
803 for 85 traits ranging from the molecular to the whole-plant level. *New Phytologist* **233**: 1560–
804 1596.
- 805 Prentice IC, Dong N, Gleason SM, Maire V, Wright IJ. 2014. Balancing the costs of carbon
806 gain and water transport: testing a new theoretical framework for plant functional ecology.
807 *Ecology Letters* **17**: 82–91.
- 808 Prentice IC, Liang X, Medlyn BE, Wang Y-P. 2015. Reliable, robust and realistic: The three
809 R's of next-generation land-surface modelling. *Atmospheric Chemistry and Physics* **15**: 5987–
810 6005.
- 811 R Core Team. 2021. R: A language and environment for statistical computing.
- 812 Rastetter EB, Vitousek PM, Field CB, Shaver GR, Herbert D, Ågren GI. 2001. Resource
813 optimization and symbiotic nitrogen fixation. *Ecosystems* **4**: 369–388.
- 814 Reich PB, Hobbie SE, Lee T, Ellsworth DS, West JB, Tilman D, Knops JMH, Naeem S,
815 Trost J. 2006. Nitrogen limitation constrains sustainability of ecosystem response to CO₂.
816 *Nature* **440**: 922–925.
- 817 Rogers A, Medlyn BE, Dukes JS, Bonan GB, Caemmerer S, Dietze MC, Kattge J, Leakey
818 ADB, Mercado LM, Niinemets Ü, et al. 2017. A roadmap for improving the representation of
819 photosynthesis in Earth system models. *New Phytologist* **213**: 22–42.
- 820 Saathoff AJ, Welles J. 2021. Gas exchange measurements in the unsteady state. *Plant Cell and
821 Environment* **44**: 3509–3523.
- 822 Schneider CA, Rasband WS, Eliceiri KW. 2012. NIH Image to ImageJ: 25 years of image
823 analysis. *Nature Methods* **9**: 671–675.

- 824 **Smith NG, Dukes JS.** 2013. Plant respiration and photosynthesis in global-scale models:
825 incorporating acclimation to temperature and CO₂. *Global Change Biology* **19**: 45–63.
826 **Smith NG, Keenan TF.** 2020. Mechanisms underlying leaf photosynthetic acclimation to
827 warming and elevated CO₂ as inferred from least-cost optimality theory. *Global Change Biology*
828 **26**: 5202–5216.
829 **Smith NG, Keenan TF, Prentice IC, Wang H, Wright IJ, Niinemets Ü, Crous KY,**
830 **Domingues TF, Guerrieri R, Ishida FY, et al.** 2019. Global photosynthetic capacity is
831 optimized to the environment. *Ecology Letters* **22**: 506–517.
832 **Taylor BN, Menge DNL.** 2018. Light regulates tropical symbiotic nitrogen fixation more
833 strongly than soil nitrogen. *Nature Plants* **4**: 655–661.
834 **Terrer C, Vicca S, Stocker BD, Hungate BA, Phillips RP, Reich PB, Finzi AC, Prentice IC.**
835 2018. Ecosystem responses to elevated CO₂ governed by plant–soil interactions and the cost of
836 nitrogen acquisition. *New Phytologist* **217**: 507–522.
837 **Walker AP, Beckerman AP, Gu L, Kattge J, Cernusak LA, Domingues TF, Scales JC,**
838 **Wohlfahrt G, Wullschleger SD, Woodward FI.** 2014. The relationship of leaf photosynthetic
839 traits - V_{cmax} and J_{max} - to leaf nitrogen, leaf phosphorus, and specific leaf area: a meta-analysis
840 and modeling study. *Ecology and Evolution* **4**: 3218–3235.
841 **Wang H, Prentice IC, Keenan TF, Davis TW, Wright IJ, Cornwell WK, Evans BJ, Peng C.**
842 2017. Towards a universal model for carbon dioxide uptake by plants. *Nature Plants* **3**: 734–741.
843 **Waring EF, Perkowski EA, Smith NG.** 2023. Soil nitrogen fertilization reduces relative leaf
844 nitrogen allocation to photosynthesis. *Journal of Experimental Botany* **74**: 5166–5180.
845 **Wellburn AR.** 1994. The spectral determination of chlorophylls a and b, as well as total
846 carotenoids, using various solvents with spectrophotometers of different resolution. *Journal of*
847 *Plant Physiology* **144**: 307–313.
848 **Wieder WR, Cleveland CC, Smith WK, Todd-Brown K.** 2015. Future productivity and
849 carbon storage limited by terrestrial nutrient availability. *Nature Geoscience* **8**: 441–444.
850 **Wright IJ, Reich PB, Westoby M.** 2003. Least-cost input mixtures of water and nitrogen for
851 photosynthesis. *The American Naturalist* **161**: 98–111.
852